Mecánica Computacional Vol. XXII
M. B. Rosales, V. H. Cortínez y D. V. Bambill (Editores)
Bahía Blanca, Argentina, Noviembre 2003.

NATURAL CONVECTION WITH TURBULENT FLOW IN A RECTANGULAR CAVITY WITH COOLED SURFACES

Rogerio Fernandes Brito[*], Paulo Mohallem Guimarães[**], Genesio Jose Menon[***]

Department of Mechanical Engineering, Federal University of Itajuba – UNIFEI
BPS Avenue, #1303 – Zip Code: 37500-176 – Itajuba, MG – Brazil. Phone: 55-35-3629-1163
e-mail: [*]rogbrito@unifei.edu.br; [**]paulomgui@uol.com.br; [***]genesio@iem.efei.br,
web page: http://www.unifei.edu.br/

Key words: Cavities, Finite Element, Turbulence, Natural Convection, LES.

Abstract. *It is studied in the present work the natural convection of the air ($Pr = 0.7$), in a rectangular cavity in order to evaluate the heat gain of the domain. It is considered a rectangular cavity whose upper surface is kept at a cold isothermal temperature and the remaining walls at constant convection. To discretize the computational domain, the Galerkin finite element method is applied. The flow is considered to be two-dimensional, turbulent, incompressible, and unsteady. In the turbulence model, it is implemented the large eddy simulation (LES) with two sub-grid scale models: vorticity transfer theory (VTT) and second-order structure-function (F2). The streamfunction ψ, the temperature θ, and the velocity vectors are obtained. The average Nusselt numbers Nu_m are also calculated on the vertical surfaces as a function of some geometrical and physical parameters.*

1 INTRODUCTION

Transient natural convection flows occur in many technological and industrial applications. On natural convection process the buoyancy forces appear due to density variation and this can influence the heat transfer. Therefore, it is important to understand the heat transfer characteristics of natural convection in an enclosure.

On the other hand, some studies on the reduction of the energy consumption have been carried out in the last years. The goals of these works have been to lower costs and improve the efficiency of domestic, industrial, and commercial equipments.

It is known that the major part of the electrical energy produced in a country is addressed to the domestic use and that one third of it is spent with refrigeration systems. Hence, it is important to study the domestic coolers that are strongly responsible, together with showers, for the electrical energy consumption in our homes. Therefore, it is appealing to verify the temperature field in a room submitted to a turbulent flow that gains heat from an external environment.

In the present work, a two-dimensional numerical simulation in a cavity with a cold upper wall is carried out for a turbulent flow. The turbulence study is a complex and challenging assumption. There are few works in the literature that deals with natural convection in closed cavities using the turbulence model LES. The motivation to accomplish this work relies on the fact that a great amount of problems in engineering that can use this geometry. Two turbulence models are implemented here together with the finite element method.

A large eddy simulation (LES) seems a promising approach for the analysis of the high Grashof number turbulence that contains three-dimensional and unsteady characteristics. A direct simulation of turbulence gives us more accurate and precise data than experiments; it is essentially unsuitable for the high Grashof number flows because of computational limitations. It is known that the LES enables an accurate prediction of turbulence, but spends much less CPU time than the direct simulation.

In the literature, a large number of theoretical and experimental investigations are reported on natural convection in enclosures.

Bispo et all[1] (1996) studied turbulent natural convection in a cavity simulating an evaporator. On the upper horizontal surface, isotherm temperature was imposed and on the other surfaces, a constant convection boundary condition was defined.

Cesini et all[4] (1999) have analyzed the natural convection heat transfer from a horizontal heated cylinder enclosed in a rectangular cavity. In that work, conductive heat transfer through the upper horizontal wall was imposed. The flow was considered laminar.

Peng and Davidson[13] (1999) used the finite volume method with the k-ω model to study flows with thermal stratification using turbulence models for low Reynolds numbers. Smoothing functions were applied to eliminate the problem of mesh dependency giving rise to correct asymptotic behavior near the wall. The geometry was a cavity with aspect ratio $A = 5$ and Rayleigh number $Ra = 5 \times 10^{10}$ with a heating wall temperature $T_h = 77.2$ [^oC] and cooling wall temperature $T_c = 31.4$ [^oC].

Peng and Davidson[14] (2001) studied the turbulent natural convection in a closed enclosure whose vertical lateral walls were maintained at different temperatures. Both the Smagorinsk and the dynamic models were applied to the turbulence simulation. Peng and Davidson[14] (2001) modified the Smagorinsk model by adding the buoyancy term to the turbulent viscosity calculation. This model will be called the Smagorinsk model with buoyancy term. The computed results were compared to experimental data and showed a stable thermal stratification under a low turbulence level ($Ra = 1.58 \times 10^9$).

A study on the streamfunction and temperature distributions in a refrigerator was developed by Cortella et all[5] (2001) using the finite volume method. The computational code was based on the vorticity-streamfunction formulation by incorporating the turbulent model LES, where the turbulent fluxes were estimated according to the vorticity transfer theory (VTT).

It was performed in the work of Oliveira and Menon[10] (2002a), a numerical study of turbulent natural convection in square enclosures. The finite volume method together with large eddy simulation was used. The enclosure lateral surfaces are kept to different isothermal and the upper and lower surfaces are isolated. The flow is studied for low Rayleigh numbers $Ra = 1.58 \times 10^9$. Three turbulence LES models were used.

A natural convection heat transfer study in closed rectangular enclosures was accomplished by Oliveira and Menon[11] (2002b) considering a turbulent regime and a k-ω turbulence model. The local and average Nusselt numbers were evaluated for Rayleigh numbers between 10^5 to 10^{10}. The Prandtl number was 0.71 and the aspect ratios were A = 5, 2, 1 and 0.5.

Brito et all[3] (2002) studied the natural convection heat transfer in a rectangular enclosure with an internal cylinder considering the turbulent regime. The flow was taken to be two-dimensional, incompressible, and unsteady. A large eddy simulation with sub-grid modeling and the second-order structure-function model (F2) was used. The local Nusselt number Nu was evaluated for Rayleigh number $Ra = 1.58 \times 10^9$, Prandtl number Pr = 0.7, and an aspect ratio A = 1.

Brito et all[2] (2003) conducted a numerical analysis on the turbulent natural convection in a single horizontal square cavity where the vertical lateral walls were isothermal, while the lower and upper horizontal walls were adiabatic. There was a conductive square body within the cavity. The objective of the heat transfer analysis was the investigation of the Nusselt number distribution on the vertical walls for various Rayleigh numbers. Comparisons were made not only with experimental and numerical results found in Tian and Karyiannis[17,18] (2000), Oliveira and Menon[10] (2002a), but also with the numerical studies by Lankhorst[8] (1991) and Cesini et all[4] (1999).

In the present work, it is considered a model that could be applied to fridges. The objective of the heat transfer analysis is to investigate the Nusselt number distribution on the walls of the rectangular closed cavity by using two turbulence models and two computational meshes. Four cases are studied numerically. The first case (case 1) is obtained using LES with vorticity transfer theory sub-grid scale model (VTT). In case 1, 2,934 linear triangular elements and 1,543 nodes are used. Although case 2 has the same turbulence model, the mesh is different with 5,294 elements and 2,749 nodes. Cases 3 and 4 have the same meshes as in cases 1 and 2, respectively, but the turbulence model LES is used with the second order structure function sub-grid scale model (F2). The rectangular cavity with aspect ratio A = H/L = 2.0, is cooled on the top wall and gains heat from the environment through the vertical and bottom walls. As an initial step for designing a more economic fridge, a constant convection coefficient h is taken for the vertical walls and a higher one for the bottom wall. The room temperature is given by T_∞. The lower horizontal surface S_2 has constant convective conditions in which $h_2 = 20$ [W/m^2 °C] and $T_\infty = 1$ [°C] whereas the upper one is an isothermal surface with $T_c = -1$ [°C]. The lateral vertical surfaces S_1 and S_3 have the same constant convective conditions where $h_1 = 10$ [W/m^2 °C] and $T_\infty = 1$ [°C]. Comparisons are made not only with experimental and numerical results found in Tian and Karyiannis[17, 18] (2000), Oliveira and Menon[10] (2002a), but also with the numerical studies by Lankhorst[8] (1991) and Cesini et all[4] (1999).

2 PROBLEM DESCRIPTION

Figure (1) shows the geometry with the domain Ω. It will be considered a rectangular cavity. The upper horizontal surface S_4 is isothermal with temperature T_c.= -1 [°C]. The convective boundary conditions on the vertical surfaces S_1 and S_3 have $h_1 = 10$ [W/m^2 °C] and $T_\infty = 1$ [°C]. The convective boundary conditions on the bottom horizontal surface S_2 have $h_2 = 20$ [W/m^2 °C] and $T_\infty = 1$ [°C]. The initial condition in Ω is: T = 0 with $\psi = \omega = 0$. All the physical properties of the fluid are constant except the density in the buoyancy term where it obeys the Boussinesq approximation. It is assumed that the third dimension of the cavities is large enough so that the flow and heat transfer are two-dimensional.

Figures (2a) and (2b) show the meshes used in the numerical simulations of the present work. Two meshes are used in order to verify their refinement effect on the average Nusselt numbers on the surfaces. One with 2,934 linear triangular elements and 1,543 nodes and another with 5,294 nodes and 2,749 nodes.

2.1 Problem Hypothesis

The following hypotheses are employed in the present work: unsteady regime; turbulent regime; two-dimensional flow; incompressible flow; constant fluid physical properties, except the density in the buoyancy terms.

3 TEORY OF SUB-GRID SCALE MODELLING

The governing conservation equations are:

$$\frac{\partial u_i}{\partial x_i} = 0 \tag{1}$$

$$\frac{\partial u_i}{\partial t} + \frac{\partial u_i u_j}{\partial x_j} = -\frac{1}{\rho}\frac{\partial p}{\partial x_i} + \frac{\partial}{\partial x_j}\left\{\nu\left[\frac{\partial u_i}{\partial x_j} + \frac{\partial u_j}{\partial x_i}\right]\right\} + g\beta(T - T_0)\delta_{2j}, \tag{2}$$

$$\frac{\partial T}{\partial t}+\frac{\partial u_j T}{\partial x_j}=\frac{\partial}{\partial x_j}\left[\alpha\frac{\partial T}{\partial x_j}\right]+S, \tag{3}$$

where x_i are the axial coordinates x and y, u_i are the velocity components, p is the pressure, T is the temperature, ρ is the fluid density, ν is the kinematic viscosity, g is the gravity acceleration, β is the fluid volumetric expansion coefficient, δ_{2j} is the Kronecker delta, α is the thermal diffusivity, and S the source term. The last term in Eq. (2) is the Boussinesq buoyancy term where T_0 is the reference temperature.

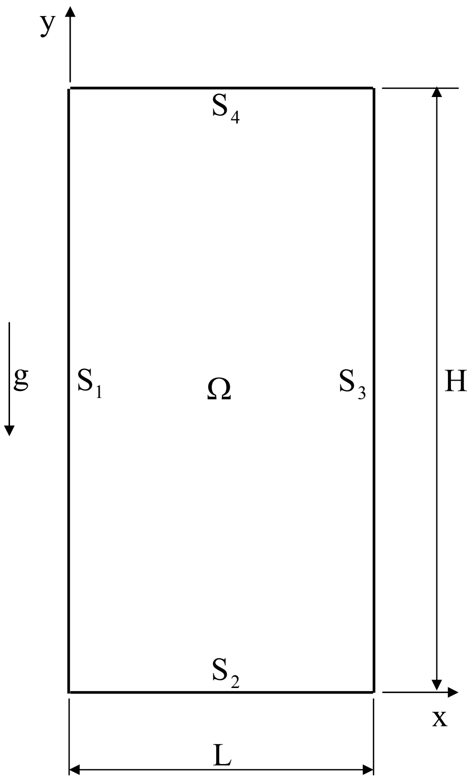

Figure 1: Cavity geometry.

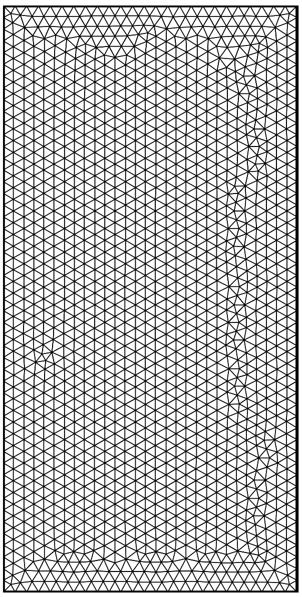

Figure 2a: Mesh arrangement 1 for cases 1 and 3.

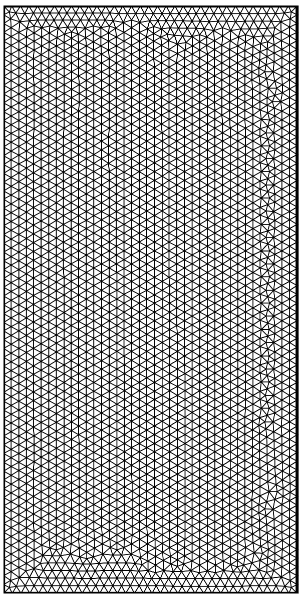

Figure 2b: Mesh arrangement 2 for cases 2 and 4.

In the large eddy simulation (LES), a variable decomposition similar to the one in the Reynolds decomposition is performed, where the quantity φ is split as follows:

$$\varphi=\overline{\varphi}+\varphi', \tag{4}$$

where $\overline{\varphi}$ is the large eddy component and φ' is the small eddy component.

The following filtered conservation equations are shown after applying the filtering operation to Eq. (1) to (3). This is done by using the volume filter function presented in Krajnovic[7] (1998). The density is constant.

$$\frac{\partial \overline{u}_i}{\partial x_i} = 0, \tag{5}$$

$$\frac{\partial \overline{u}_i}{\partial t} + \frac{\partial \overline{u_i u_j}}{\partial x_j} = -\frac{1}{\rho}\frac{\partial \overline{p}}{\partial x_i} + \frac{\partial}{\partial x_j}\left\{\nu\left[\frac{\partial \overline{u}_i}{\partial x_j} + \frac{\partial \overline{u}_j}{\partial x_i}\right]\right\} + g\beta\left(\overline{T} - T_0\right)\delta_{2j}, \tag{6}$$

$$\frac{\partial \overline{T}}{\partial t} + \frac{\partial \overline{u_j T}}{\partial x_j} = \frac{\partial}{\partial x_j}\left[\alpha \frac{\partial \overline{T}}{\partial x_j}\right] + S. \tag{7}$$

In Equations (5) to (7), $\overline{u_i u_j}$ and $\overline{u_j T}$ are the filtered variable products that describe the turbulent momentum transport and the heat transport, respectively, among the large and sub-grid scales.

According to Oliveira and Menon[10] (2002a), the products $\overline{u_i u_j}$ and $\overline{u_j T}$ are split into other terms by including the Leonard L_{ij} tensor, the Crossing tensor C_{ij},, the Reynolds sub-grid tensor R_{ij}, the Leonard turbulent flux $L_{\theta j}$, the Crossing turbulent flux $C_{\theta j}$ and the sub-grid turbulent flux θ_j. The Crossing and Leonard terms, according to Padilla[12] (2000), can be neglected. After the development shown in Oliveira and Menon[10] (2002a), the following conservation equations are obtained:

$$\frac{\partial \overline{u}_i}{\partial x_i} = 0, \tag{8}$$

$$\frac{\partial \overline{u}_i}{\partial t} + \frac{\partial\left(\overline{u}_i\, \overline{u}_j\right)}{\partial x_j} = -\frac{1}{\rho}\frac{\partial \overline{p}}{\partial x_i} + \nu\left(\frac{\partial^2 \overline{u}_i}{\partial x_j \partial x_j}\right) - \frac{\partial \tau_{ij}}{\partial x_i} + g\beta\left(\overline{T} - T_0\right)\delta_{2j}, \tag{9}$$

$$\frac{\partial \overline{T}}{\partial t} + \frac{\partial\left(\overline{u}_j \overline{T}\right)}{\partial x_j} = \frac{\partial}{\partial x_j}\left[\alpha \frac{\partial \overline{T}}{\partial x_j}\right] + \frac{\partial \theta_j}{\partial x_j}. \tag{10}$$

where, Pr is the Prandtl number with $\alpha = \nu/Pr$. The tensors τ_{ij} and θ_j that appear in Eq. (9) and (10) are modeled in the forthcoming topics.

3.1 Sub-grid scale model

Many sub-grid scale models use the diffusion gradient hypothesis similar to the Boussinesq one that expresses the sub-grid Reynolds tensor in function of the deformation rate and kinematic energy. According to Silveira-Neto[15] (1998), the Reynolds tensor is defined as:

$$\tau_{ij} = -2\nu_T \overline{S}_{ij} - \frac{2}{3}\delta_{ij}\overline{S}_{kk}, \tag{11}$$

where, ν_T is the turbulent kinematic viscosity, δ_{ij} is the Kronecker delta and $\overline{S}_{ij}$ is deformation tensor rate given by:

$$\overline{S}_{ij} = \left(\frac{\partial \overline{u}_i}{\partial x_j} + \frac{\partial \overline{u}_j}{\partial x_i}\right). \tag{12}$$

Substituting $\overline{S}_{ij}$ in Eq. (9):

$$\frac{\partial \overline{u}_i}{\partial t} + \frac{\partial\left(\overline{u}_i\,\overline{u}_j\right)}{\partial x_j} = -\frac{1}{\rho}\frac{\partial \overline{P}}{\partial x_i} + \nu\left(\frac{\partial^2 \overline{u}_i}{\partial x_j \partial x_j}\right) + \frac{\partial}{\partial x_j}\left\{\nu_T\left[\frac{\partial \overline{u}_i}{\partial x_j} + \frac{\partial \overline{u}_j}{\partial x_i}\right]\right\} + g\beta\left(\overline{T} - T_0\right)\delta_{2j}. \tag{13}$$

In a similar way, the energy equation is obtained:

$$\frac{\partial \overline{T}}{\partial t} + \frac{\partial\left(\overline{u}_j \overline{T}\right)}{\partial x_j} = \frac{\partial}{\partial x_j}\left[\left(\alpha + \alpha_T\right)\frac{\partial \overline{T}}{\partial x_j}\right]. \tag{14}$$

where the turbulent thermal diffusivity is calculated as:

$$\alpha_T = \nu_T / Pr_T, \tag{15}$$

and Pr_T is the turbulent Prandtl number.

The sub-grid models propose the following expression for the turbulent viscosity ν_t:

$$\nu_T = c\,\ell\,q, \tag{16}$$

where c is a dimensionless constant, ℓ and q are the scale lengths and the velocity, respectively.

The parameter ℓ is related to the filter size and it is usually used in the two-dimensional case with a rectangular element as:

$$\ell = \overline{\Delta} = \left(\Delta_1 \Delta_2\right)^{1/2}, \tag{17}$$

where Δ_1 and Δ_2 are the filter lengths in x and y directions.

3.1.1 The second-order structure-function sub-grid scale model (F2)

In cases 3 and 4, the element turbulent viscosity is calculated at the element centroid regarding the velocities of the neighboring element centroids. As a two-dimensional numerical simulation is performed, an adaptation of the velocity structure function F2, which is used in the turbulent viscosity ν_T, is needed. In a 3D model, the velocities of the neighboring elements are calculated within a sphere of a previously calculated radius R. As for the 2D model, these same velocities are calculated within a circle of radius R. Each element from the neighborhood has its centroid located in a distance smaller or equal than the value R of a circumference reaching those neighboring elements. R is given by R = γ (a + b + c)/3, where a, b, and c are distances of the centroid to the element vertexes and γ is adopted as 1,9.

The turbulent viscosity ν_T is calculated as follows:

$$\nu_T(\vec{x},\Delta,t) = 0.104\, C_k^{-3/2}\, \Delta \sqrt{\overline{F}_2(\vec{x},\Delta,t)}\,, \tag{18}$$

where C_k = 1.4 is the Kolmogorov constant (Kolmogorov[6], 1941). The variable Δ is the geometric average of the distances d_i from the neighboring elements to the point where ν_T is calculated and is given by:

$$\Delta = \sqrt[N]{\prod_{i=1}^{N} d_i}\ , \tag{19}$$

and $\overline{F}_2(\vec{x},\Delta,t)$ is the structure function of second order velocities.

According to Kolmogoroy[6], 1941 law that establishes that the structure function of second order velocities is proportional to $(\varepsilon r)^{2/3}$, where r is the distance between two points, the structure function can be calculated as:

$$\overline{F}_2 = \frac{1}{N}\sum_{i=1}^{N}\left\{\left\{\left[u_i\left(\vec{x}+d_i\,\vec{e}_i,t\right)-u\left(\vec{x},t\right)\right]^2+\left[\upsilon_i\left(\vec{x}+d_i\,\vec{e}_i,t\right)-\upsilon\left(\vec{x},t\right)\right]^2\right\}\left(\frac{\Delta}{d_i}\right)^{2/3}\right\}\,, \tag{20}$$

where $u_i(\vec{x}+d_i\,\vec{e}_i,t)$ and $\upsilon_i(\vec{x}+d_i\,\vec{e}_i,t)$ are the velocities at the point "i" of the neighboring centroid placed at a distance d_i from the target point, $u(\vec{x},t)$ and $\upsilon(\vec{x},t)$ are the velocities at this point of the element, N is the number of points from the neighborhood, t is the time and $\vec{e}_i$ the vector on the d_i direction.

3.1.2 Vorticity transfer theory of sub-grid scale model (VTT)

In cases 1 and 2, the turbulence model implemented can be classified as a large eddy simulation (LES), according to Cortella et all[5] (2001), where the turbulent fluxes are estimated on the basis of the vorticity transfer theory (VTT). In accordance with this approach, the turbulent kinematic viscosity is computed as:

$$\nu_T = (C\Delta)^3\left[\left(\frac{\partial\omega}{\partial x}\right)^2+\left(\frac{\partial\omega}{\partial y}\right)^2\right]^{1/2}, \tag{21}$$

where ω is the vorticity and Δ is the average dimension of the element given by:

$$\omega = \frac{\partial v}{\partial x} - \frac{\partial u}{\partial y} \text{ and } \Delta = \left(\prod_{k=1}^{N} d_k \right)^{1/N} . \tag{22}$$

where, $\vec{x}$ is the position vector of the center of the reference element and d_k (k = 1 to N), the distance from the center of the reference element to the center of the neighbor element. More details on this model can be seen on the work of Métais e Lesieur[9] (1996).

For isotropic turbulence, the dimensionless constant C = 0.2 can be satisfactorily used according to Cortella et all[5] (2001). The turbulent thermal diffusion is estimated from the turbulent kinematic viscosity, by assuming:

$$Pr_T = \nu_T / \alpha_T = 0.4 . \tag{23}$$

4 INITIAL AND BOUNDARY CONDITIONS

From this section on, the upper bars that mean the average values $\overline{T}$ and $\overline{u}$ will be omitted.

Figure (1) pictures the enclosure on which the initial conditions are imposed:

$$u(x,y,0) = 0,\ v(x,y,0) = 0,\ T(x,y,0) = 0 , \qquad \text{in } \Omega, \tag{24}$$

The boundary conditions imposed are:

$$u = v = 0,\ T_\infty = 1,\ h_1 = 10, \qquad \text{on } S_1, \tag{25}$$

$$u = v = 0,\ T_\infty = 1,\ h_2 = 20, \qquad \text{on } S_2, \tag{26}$$

$$u = v = 0,\ T_\infty = 1,\ h_1 = 10, \qquad \text{on } S_3, \tag{27}$$

$$u = v = 0,\ T = T_c = -1, \qquad \text{on } S_4, \tag{28}$$

Besides that, the flow field can be described by the streamfunction ψ and the vorticity ω distributions given by:

$$u = \partial\psi/\partial y ,\ \upsilon = -\partial\psi/\partial x ,\ \omega = (\partial\upsilon/\partial x) - (\partial u/\partial y), \tag{29}$$

where u and υ are the velocity components in the x and y directions , respectively. Hence, the continuity equation given by Eq. (1), is exactly satisfied. Working with dimensionless variables, it is possible to deal with Rayleigh number Ra, Prandtl number Pr and the enclosure aspect ratio A given by:

$$Ra = Pr\left[g\beta(T_h - T_c)H^3/\nu^2 \right] = 1.58 \times 10^9 \ ,\ Pr = \nu/\alpha = 0.7 \ ,\ A = H/L = 2.0 , \tag{30}$$

where T_∞ and T_c are the room temperature and the temperature on S_4, respectively. H is a characteristic dimension.

5 NUMERICAL METHOD

Equations (8) to (10) are solved through the finite element method (FEM) with a linear triangular element. The discretization uses the Galerkin formulation. The system of equations is solved with the Gauss Quadrature. The problem solution follows the steps below:

($1^{\underline{0}}$) through Eq. (29) the streamfunction field ψ is solved; ($2^{\underline{0}}$) the wall vorticity is determined in matricial form, according to Silveira-Neto et all[16] (2000); ($3^{\underline{0}}$) the boundary conditons for vorticity are applied; ($4^{\underline{0}}$) the vorticity in the interior is calculated according to Eq. (29); ($5^{\underline{0}}$) the temperature field is solved through Eq. (10); ($6^{\underline{0}}$) the local Nusselt is obtained using Eq. (31); ($7^{\underline{0}}$) the time is increased with the time step Δt and the iteration with unity and then it turns to the first step ($1^{\underline{0}}$) starting all over again till it reaches the stop criterion. The local Nusselt number Nu is defined as:

$$Nu = \left(\partial T/\partial n\right)_w H/\left(T_\infty - T_c\right). \tag{31}$$

where n is the unit vector normal to the surface or boundary where the local Nusselt number Nu is calculated.

6 NUMERICAL METHOD VALIDATION

In order to compare the results with the ones found in the literature and then to validate the computational code in FORTRAN, two cases are taken from Brito et all[3] (2002) and Brito et all[2] (2003). Brito et all[3] (2002) and Brito et all[2] (2003) use the same turbulence model LES as the one used in the present work. In the first comparison, the study of the natural turbulent flow in a square enclosure with different temperatures for various Rayleigh numbers is carried out in Brito et all[3] (2002). The second comparison is made in the Brito et all[2] (2003)´s work considering a laminar flow in a rectangular enclosure with an internal cylinder.

In the first comparison, it is also used the large eddy simulation (LES). The results in Brito et all[3] (2002) are compared not only to the experimental and numerical ones in Peng and Davidson[13] (2001), but also to the numerical ones in Lankhorst[8] (1991). A good agreement is verified. It is also made a comparison between the results from Brito et all[3] (2002), for the average dimensionless temperature and the experimental ones given by Tian and Karayiannis[17, 18] (2000).

The second comparison is made in Brito et all[2] (2003) whose results are compared to the ones in Cesini et all[4] (1999). Cesini et all[4] (1999) considered a two-dimensional laminar flow. For the numerical simulation made by Cesini et all[4] (1999), a dimension z is adopted in such a way that the flow can be considered two-dimensional. Cesini et all[4] (1999) study a rectangular enclosure where the horizontal surface has a constant convection heat transfer whereas the horizontal lower surface is submitted to isolation. The vertical surfaces are isothermal having a low temperature T_c. On the other hand, the cylinder surface has a high temperature T_h. In the second comparison, the maximum deviation is 11.88 % with Rayleigh number equal to

3.4×10^3 using a mesh with 5,790 elements and 3,011 node points. The minor deviation is 7.53 % to Rayleigh number equal to 3.0×10^4.

7 RESULTS

The objectives of the present numerical work are: verify the influence of the mesh refinement and of the different turbulent models LES with sub-grid scale modelling on the domain considered here.The flow is considered turbulent with $Ra = 1.58 \times 10^9$ and $Pr = 0.7$. The geometry parameters used in the four cases mentioned previously are: $H = 1$; $L = 0.5$; $T_\infty = 1$; $T_c = -1$; $A = H/L = 2.0$; $h_1 = 10$ and $h_2 = 20$.

Figure 3 presents the local Nusselt number Nu on surface S_1 with $Ra= 1.58 \times 10^9$ for all cases. It is noted from Fig. (3) that Nu varies along S_1, but with similar results for the cases despite the meshes and the turbulence models. Only in case 2, for $Y \approx 0.8$, there is a higher peak on the local Nusselt number. The Nusselt numbers Nu obtained on the vertical surface S_1 are lower than the ones on the horizontal surface S_4, due to on S_4 a constant convection is imposed instead of an isothermal temperature.

Figures 4, 5, 6, and 7 present the results for the average Nusselt numbers Nu_m on S_1, S_2, S_3 and S_4 versus time t for cases 1, 2, 3, and 4, respectively. Figures 4 and 5 use the same turbulence model LES with vorticity transfer theory (VTT). In case 2, Fig. 5, the mesh refinement make Nu_m be higher along the time, mainly on the horizontal surface S_4.

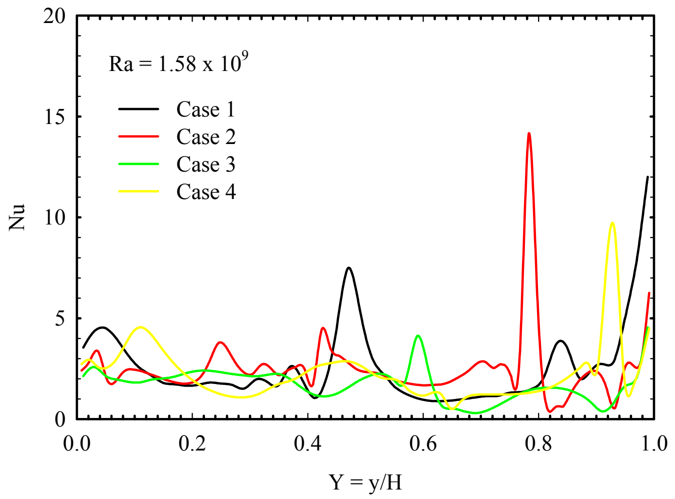

Figure 3: Local Nusselt number on S_1 for $Ra = 1.58 \times 10^9$ and $t = 600\ t_0$.

This was already expected in a certain way because the mesh refinement gives more accurate results. On the other hand, the variation of Nu_m the time happens due to the fact that in LES, the results do not reflect an average amount, but all the physical instabilities in the flow.

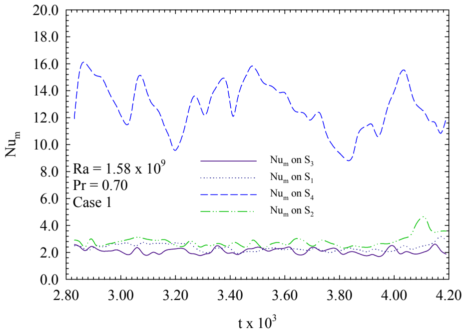

Figure 4: Nu_m versus t for case 1.

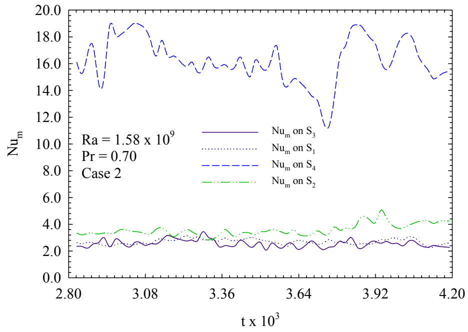

Figure 5: Nu_m versus t for case 2.

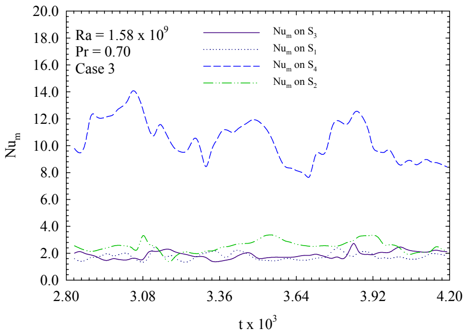

Figure 6: Nu_m versus t for case 3.

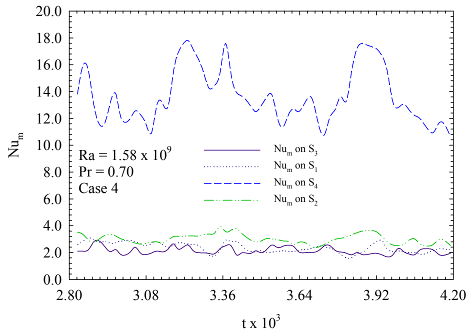

Figure 7: Nu_m versus t for case 4.

Figures 4, 5, 6 and 7: Average Nusselt number Nu_m on S_1, S_2, S_3 and S_4 for Pr = 0.7, Ra = 1.58×10^9 and t = (400-600)t_0.

Figures 6 and 7 present Nu_m versus time t for all the surfaces in the rectangular cavity. The turbulence model with the second-order structure-function sub-grid scale (F2) is used. It is observed that the behavior of the curves is similar to the one in Fig. 4 and 5. Comparing Figs. 6 and 7, that is, cases 3 and 4, respectively, the mesh refinement gives again different and bigger values for Nu_m.

Contrasting now the results for Nu_m obtained with different sub-grid-models according to Figs. 5 and 7, it is noted that Nu_m for S_1, S_2 , and S_3 are quite similar. Nu_m on S_4, for a period of time t = 2.83 x 10^{-3} to 3.23 x 10^{-3}, showed to have the largest difference.

Figure 8 brings the streamfunction ψ, the average temperature T_m distributions and the velocity vectors for Ra = 1.58×10^9 and Pr = 0.70 for case 1. There are three major recirculations inside the cavity. A hotter fluid region appears near the horizontal bottom wall due to the heat gain from the outside that is imposed by the constant convection boundary condition.

Figure 9 brings the streamfunction ψ, the average temperature T_m distributions and the velocity vectors for Ra = 1.58×10^9 and Pr = 0.70 for case 2. With the mesh refinement, the recirculation regions are more defined and the fluid region with higher temperature is larger than the one in Fig. 8.

Figure 10 brings the streamfunction ψ, the average temperature T_m distributions and the velocity vectors for Ra = 1.58×10^9 and Pr = 0.70 for case 3. The mesh used here is the same as in case 1. The turbulence model is LES with F2. The positions of the fluid recirculations change in relation to cases 1 and 2 in Figs. 8 and 9. From Fig. 10, it is observed a fluid region on the lower right side with higher temperatures.

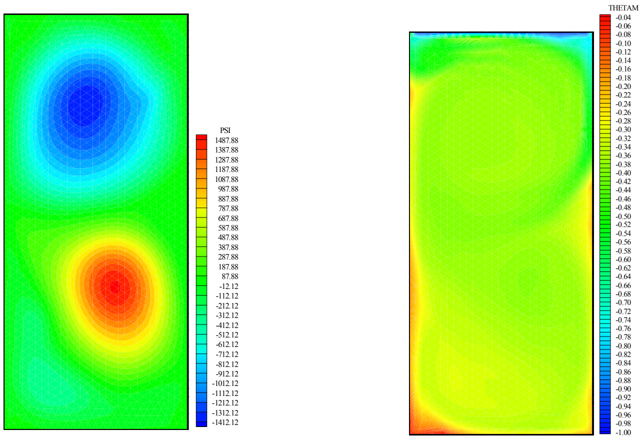

Figure 8: Case 1 - Streamfunction ψ for t = 600 t_0 ($\Delta\psi$ = 100), average temperature T_m (ΔT_m = 0.01) for t = (400-600)t_0 and velocity vectors for t = (400-600)t_0.

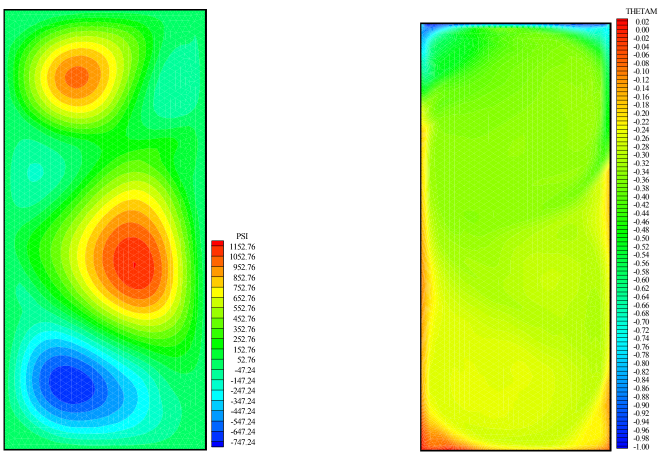

Figure 9: Case 2 - Streamfunction ψ for t = 600 t_0 ($\Delta\psi$ = 100), average temperature T_m (ΔT_m = 0.01) for t = (400-600)t_0 and velocity vectors for t = (400-600)t_0.

Figure 11 brings the streamfunction ψ, the average temperature T_m distributions and the velocity vectors for Ra = 1.58×10^9 and Pr = 0.70 for case 4. The results from case 4 are quite similar to the ones in case 3 in relation to ψ, T_m, and the velocity vectors.

8 DISCUSSION

In this work, the turbulent natural convection in a rectangular enclosure is studied with boundary conditions of isothermal temperature and constant element convection.

Two kinds of sub-grid scale models are used: large-eddy simulation (LES) with the vorticity transfer theory of sub-grid scale model (VTT) according to Cortella et all[5] (2001) and

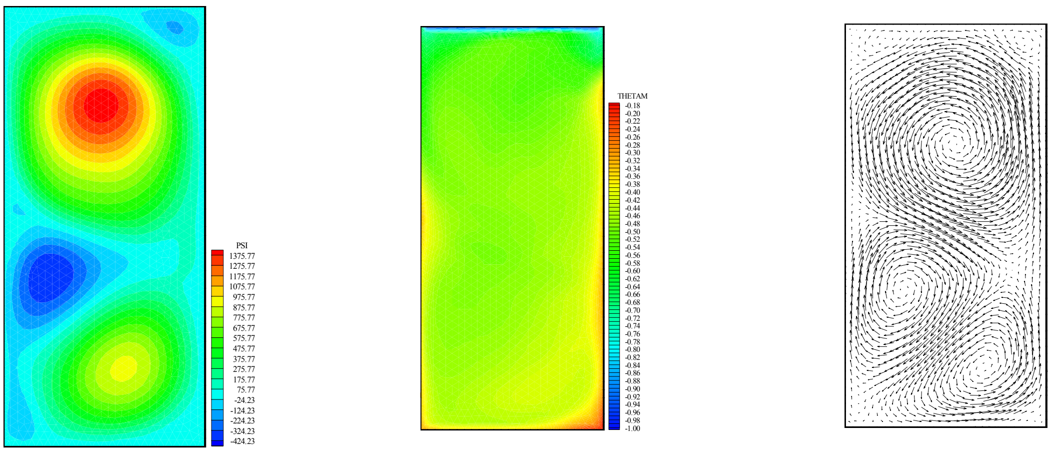

Figure 10: Case 3 - Streamfunction ψ for $t = 600\ t_0$ ($\Delta\psi = 100$), average temperature T_m ($\Delta T_m = 0.01$) for $t = (400\text{-}600)t_0$ and velocity vectors for $t = (400\text{-}600)t_0$.

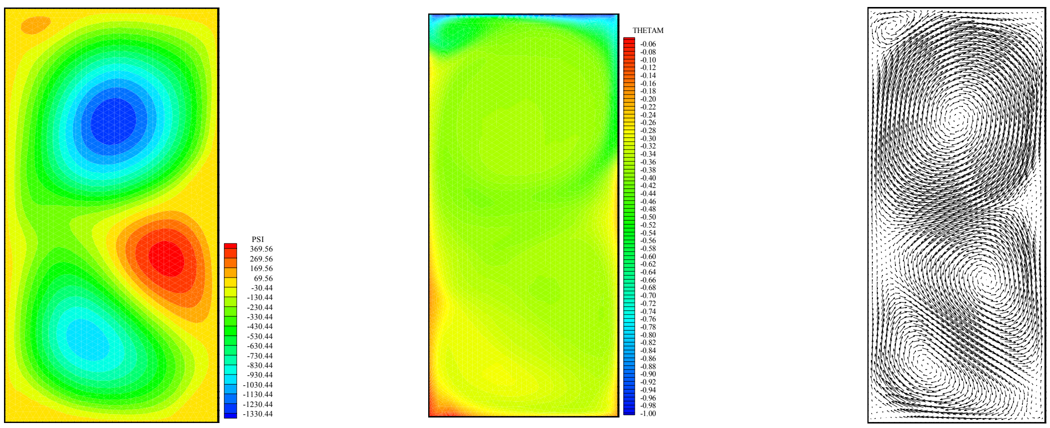

Figure 11: Case 4 - Streamfunction ψ for $t = 600\ t_0$ ($\Delta\psi = 100$), average temperature T_m ($\Delta T_m = 0.01$) for $t = (400\text{-}600)t_0$ and velocity vectors for $t = (400\text{-}600)t_0$.

LES with the second-order structure-function sub-grid scale model (F2) (more details in Silveira-Neto[15], 1998) The conservation equations are discretized by the Galerkin finite element method with linear triangular elements.

Two cases are used for validation of the computational domain of the present work. In Brito et all[3] (2002) and Brito et all[2] (2003), the same turbulence model LES, together with the finite element method, is used in the present work.

For $Ra = 1.58 \times 10^9$, it is not found a meaningful change of the average Nusselt number Nu_m on all the surfaces. Only on the upper horizontal surface S_4 there is a little difference on the average Nusselt number Nu_m. It can be noted through an animation of the streamfunction ψ and the time average temperature T_m that this complex flow does not reach the steady regime, as expected.

The streamfunction, average temperature distributions and velocity vectors are presented for Rayleigh number $Ra = 1.58 \times 10^9$ and Prandtl number $Pr = 0.7$ for $t = (400\text{-}600)t_0$.

9 ACKNOWLEDGEMENTS

The authors thank the financial support from CNPq without which this work would be impossible.

10 REFERENCES

[1] Bispo, D. J., Nieckele, A. O. and Braga, S. L., "Convecção Natural em uma Cavidade Retangular Resfriada na Parede Superior", Proceedings of the VI Congresso Brasileiro de Engenharia e Ciências Térmicas – ENCIT, VI LATCYM, Brazil, 1339-1344 (1996).

[2] Brito, R. F., Guimarães, P. M., Silveira-Neto, A., Oliveira, M. and Menon, G. J., "Turbulent Natural Convection in a Rectangular Enclosure using Large Eddy Simulation", Proceedings of the 17th International Congress of Mechanical Engineering – COBEM – São Paulo – Brazil, (2003).

[3] Brito, R. F., Silveira-Neto, A., Oliveira, M. and Menon, G. J., "Convecção Natural Turbulenta em Cavidade Retangular com um Cilindro Interno", Proceedings of the first South-American Congress on Computational Mechanics - MECOM - III Brazilian Congress on Computational Mechanics - VII Argentine Congress on Computational Mechanics - Santa Fe-Paraná – Argentina, (2002).

[4] Cesini, G., Paroncini, M., Cortella G. and Manzan, M., "Natural Convection from a Horizontal Cylinder in a Rectangular Cavity", *International Journal of Heat and Mass Transfer*, **42**, 1801-1811 (1999).

[5] Cortella, G., Manzan, M. and Comini, G., "CFD Simulation of Refrigerated Display Cabinets", *Int. J. Refrigeration*, **24**, 250-260 (2001).

[6] Kolmogorov, A. N., "The Local Structure of Turbulence in Incompressible Viscous Fluid for Very Large Reynolds Numbers", *Dokl. Akad. Nauk SSSR*, **30**, 301-305 (1941).

[7] Krajnovic, S., "Large-Eddy Simulation of the Flow Around a Surface Mounted Single Cube in a Channel", Thesis for the degree of Master of Science, Chalmers University of Technology, Goteborg, Sweden, (1998).

[8] Lankhorst, A. M., "Laminar and Turbulent Natural Convection in Cavities – Numerical

Modelling and Experimental Validation", Ph.D. Thesis, Technology University of Delft, The Netherlands, (1991).

[9] Métais, O. and Lesieur, M., "Spectral and Large-Eddy Simulation of Isotropic and Stably-Stratified Turbulence", *J. Fluid Mech*., **239**, 157-194 (1996).

[10] Oliveira, M. and Menon, G. J., "Simulação de grandes escalas utilizada para convecção natural turbulenta em cavidades", Proceedings of the 9th Congresso Brasileiro de Engenharia e Ciências Térmicas - ENCIT-2002, Caxambu - Brazil, CD ROM, 1-11 (2002a).

[11] Oliveira, M. and Menon, G. J., "Convecção Natural Turbulenta em Cavidades Retangulares", Proceedings of the II Congresso Nacional de Engenharia Mecânica - CONEM, João Pessoa - Brazil, 1-10, 2002b.

[12] Padilla, E. L. M., "Simulação Numérica de Grandes Escalas com Modelagem Dinâmica, Aplicada à Convecção Mista", Thesis for the degree of Master of Science, DEEME-UFU, Uberlândia, Brazil, 2000.

[13] Peng, S. H. and Davidson, L., "Computation of Turbulent Buoyant in Enclosures with Low-Reynolds-Number k-ω Models", *Int. J. Heat and Mass Transfer*, **20**, 172-184 (1999).

[14] Peng, S. H. and Davidson, L., "Large-Eddy Simulation for Turbulent Buoyant Flow in a Confined Cavity", *Int. J. Heat and Fluid Flow*, **22**, 323-331 (2001).

[15] Silveira-Neto, A., "Simulação de Grandes Escalas de Escoamentos Turbulentos", Proceedings of the I Escola de Primavera de Transição e Turbulência, **1**, Rio de Janeiro, Brazil, 157-190, (1998).

[16] Silveira-Neto, A., Brito, R. F., Dias, J. B. and Menon, G. J., "Aplicação da Simulação de Grandes Escalas no Método de Elementos Finitos para Modelar Escoamentos Turbulentos", Proceedings of 2nd ETT – Escola Brasileira de Primavera, Transição e Turbulência, Uberlândia, Brazil, 515-526, (2000).

[17] Tian, Y. S. and Karayiannis, T. G., "Low turbulence natural convection in an air filled square cavity part I: the thermal and fluid flow fields", *Int. J. Heat and Mass Transfer*, **43**, 849-866 (2000a).

[18] Tian, Y. S. and Karayiannis, T. G., "Low Turbulence Natural Convection in an Air Filled Square Cavity - Part II: the Turbulence Quantities", *Int. J. Heat and Mass Transfer*, **43**, 867-884 (2000b).